

Direct Calculation of Solid–Liquid Interfacial Free Energy for Molecular Systems: TIP4P Ice–Water Interface

Supplementary Information

Richard Handel and Ruslan L. Davidchack

Department of Mathematics, University of Leicester, Leicester, LE1 7RH, UK

Jamshed Anwar and Andrey Brukhno

*Computational Laboratory, Institute of Pharmaceutical Innovation,
University of Bradford, West Yorkshire BD7 1DP, UK*

(Dated: November 2, 2007)

PACS numbers: 68.08.-p,64.70.Dv,05.70.Np,87.15.Aa

INTRODUCTION

We provide here more detailed information on the following topics:

- Determination of ice I_h –water coexistence conditions for the TIP4P model with 10\AA interaction cutoff (both van der Waals and electrostatic);
- Nonequilibrium measurements approach for computing reversible work;
- Detailed discussion of the large hysteresis in Step 2 and of our approach for reducing the hysteresis
- Number and simulation time of forward and reverse trajectories.

COEXISTENCE CONDITIONS

In order to determine the coexistence conditions for our model of water (TIP4P with 10\AA interaction cutoff), we employed the direct coexistence simulation method [1–3]. In this method a heterogeneous system containing the two phases separated by an interface is allowed to evolve in a long simulation run. If the conditions of the simulation are not close to the coexistence conditions for the two phases, the system will evolve towards the phase which is more stable (i.e. the one with the lowest free energy), with the transformation between the phases taking place at the interface. In the system containing crystal and melt phases, one would observe melting (freezing) at the interface if the temperature were above (below) the melting temperature. The simulation can be carried out in a variety of ensembles: NVT, NPT, NPH (constant enthalpy).

In order to determine the ice I_h –water coexistence conditions for the TIP4P model used in our system we ran 4 ns simulations of the ice–water interfacial system at temperatures 213, 216, 219, 222, 225 K. We observed melting of the ice–water interfacial system at temperatures above 219 K (see Figure 1). As is noted in the

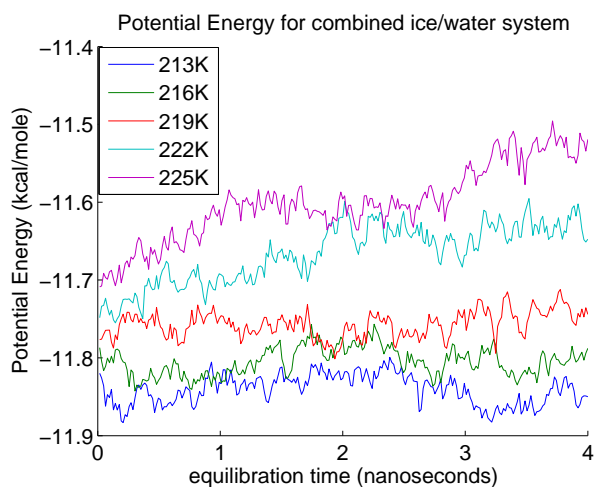


FIG. 1: Coexistence simulations at different temperatures. Each simulation starts with equal quantities of ice and water separated by interfaces. An increase (decrease) of potential energy with time indicates melting (freezing).

paper, the melting temperature of 219 K for our system is lower than those for TIP4P models reported in the literature [2–5], which were in the range 229–232 K. We attribute this to the truncation of the electrostatic interaction at 10\AA , since the higher melting temperature estimates were obtained for the TIP4P model either with full electrostatic interactions (computed via Ewald sums) [5], or with a larger interaction cutoff of 17\AA [2, 4]. To verify the effect of truncation on the melting temperature, we repeated the coexistence simulations for TIP4P with Ewald sums, and the system did not melt at 230 K.

Based on this evidence, we conclude that the truncation of electrostatic interactions in TIP4P model leads to the decrease of melting temperature. This decrease might not be noticeable with the 17\AA cutoff due to the relatively low precision of the coexistence simulation method, but it is clearly observed for the 10\AA cutoff. We are confident that our estimate of 219 K is not far from the true melting temperature for this system. In fact, if the temperature at which we performed the cleaving process were below

the melting temperature for this system, we would have ended up with an excess amount of ice at the end of the four-step cleaving process, which we did not observe.

NONEQUILIBRIUM FREE ENERGY CALCULATION METHODS

We use a nonequilibrium method to calculate work in the simulations. Since thermodynamic integration is a valid alternative, we give here some explanation of the nonequilibrium method, and discuss how it compares with thermodynamic integration, in order to justify the choice.

To calculate the free energy between two states using the nonequilibrium approach, a number of trajectories are run. The starting point for each forward trajectory is chosen at random from the *equilibrated* starting state. The trajectory then moves smoothly to the ending state. Reverse trajectories are similar – they start from a randomly chosen point in the *equilibrated* ending state, and move smoothly to the starting state. As they run, the trajectories are not in equilibrium.

To change the system state, its potential, U , is modified via a coupling parameter $\lambda(t)$, which transforms the system from its initial state, $\lambda(0) = \lambda_i$ to its final state, $\lambda(T) = \lambda_f$. The (non-equilibrium) work done is then computed [6] as:

$$W = \int_{t=0}^T \frac{\partial U(\Gamma(t); \lambda)}{\partial \lambda} \dot{\lambda}(t) dt, \quad (1)$$

where $\Gamma(t)$ represents the phase space trajectory of the system. The coupling parameter speed $\dot{\lambda} = d\lambda/dt$ can be time dependent, $\lambda(t)$, and tailored to slow the trajectory over regions where relaxation time of the system to equilibrium is relatively slow, and therefore subject to hysteresis. This ability to vary the trajectory speed is a useful device for concentrating computing time on the problematic regions of the state transition. We found a piecewise constant function adequate for this purpose, though other functions are possible.

The measurements of nonequilibrium work in both forward and reverse directions are used to determine the free energy difference between the initial and final states, ΔF , according the Bennett Acceptance Ratio (BAR) equation:

$$\sum_{i=1}^{n_F} \frac{1}{1 + e^{\beta(M+W_i - \Delta F)}} = \sum_{j=1}^{n_R} \frac{1}{1 + e^{-\beta(M+W_j - \Delta F)}}, \quad (2)$$

where $\beta = 1/k_B T$, $M = k_B T \ln(n_F/n_R)$, and n_F (n_R) is the number of forward (reverse) trajectories. This equation, originally derived by Bennett [7] for the case of instantaneous switching between two equilibrium states, has been shown [8] to be also valid when the potential energy difference between the two states is replaced with

the nonequilibrium work values for finite time switching processes in the forward and reverse directions.

As an estimator for the free energy, this equation is optimal in the statistical sense of a Maximum Likelihood Estimator [9]. The variance in the obtained value for the free energy can be estimated as follows:

$$\sigma_{\text{BAR}}^2 = \frac{1}{\beta^2 n_{\text{tot}}} \left\{ \left\langle \frac{1}{2 + 2 \cosh(\beta(M + W_i - \Delta F))} \right\rangle^{-1} - \left(\frac{n_{\text{tot}}}{n_F} + \frac{n_{\text{tot}}}{n_R} \right) \right\} \quad (3)$$

where $n_{\text{tot}} = n_F + n_R$ and the average, denoted by the angle brackets, is over all work measurements, both forward and reverse.

It is instructive to contrast this method with thermodynamic integration, which has been used in earlier studies. We have found that nonequilibrium methods provide accuracy comparable to thermodynamic integration (for given computing resources). In addition, they offer some important advantages:

Hysteresis detection: Since forward and reverse trajectories are combined in the BAR calculation, any hysteresis will show up as a significant difference between forward and reverse work, which in turn will be reflected in a high error estimate. So the method itself contains a built-in check for hysteresis.

Few equilibration runs: Within the nonequilibrium approach we need to equilibrate the system only at the initial and final states. Such states are usually far from any thermodynamic transition points and thus the equilibration is fairly rapid. To use thermodynamic integration, we need to equilibrate the system at many intermediate states. States that are close to thermodynamic transition points may exhibit weak ergodicity and thus require very long equilibration runs.

Additional trajectories can improve accuracy: If additional accuracy is required, further trajectories can be run after the initial results have been collected. The results are added to the results of the earlier trajectories, so improved accuracy can be obtained without discarding any earlier computations.

‘Naturally’ parallel computation: The free energy is calculated as an average from a number of independent trajectories. Being independent, these trajectories can be run on separate processors, enabling the simulation to be run in parallel without the need to write MPI software.

An appropriate speed for the trajectories must be established: we have found that the greatest accuracy is

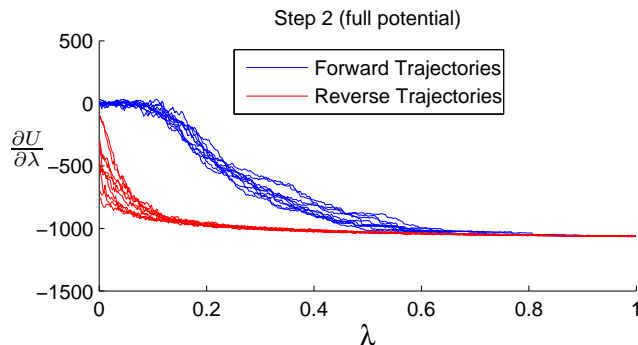


FIG. 2: Hysteresis in step 2 (cleaving water). The graph shows 10 forward and 10 reverse trajectories at co-existence conditions. Each trajectory ran for 0.9 ns. The hysteresis is too persistent to be removed by slowing down the trajectories. Free energy is impossible to calculate when the trajectories are so far from reversible.

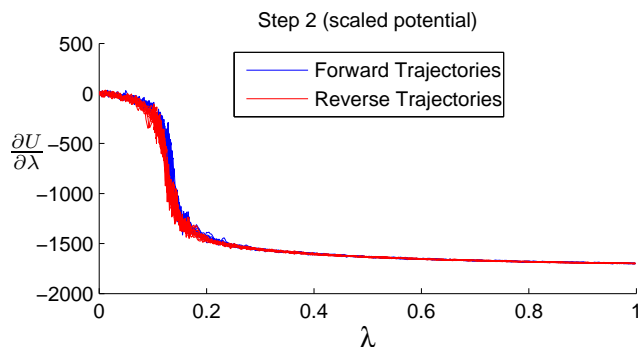


FIG. 3: Cleaving water at reduced potential. After reducing the system potential to 70% of full-strength, the hysteresis is completely removed. The forward and reverse paths are now close enough for a good estimate of the free energy to be made. The scaling and restoring of the potential are done separately (shown in the following figures).

achieved with a slow enough speed so that the system is never too far from equilibrium, so that the forward and reverse work distributions overlap somewhat.

HYSTERESIS DURING CLEAVING OF WATER (STEP 2)

As noted in previous studies [10, 11], the structural ordering of the liquid induced by the cleaving potential is the principal source of irreversibility in the cleaving method. This problem was found to be particularly severe for TIP4P water, as can be clearly seen in Figure 2. The hysteresis was found to be very persistent and could not be removed by slowing down the switching process.

The hysteresis was significantly reduced by reducing the interaction potential of the molecules. Reducing the potential, equivalent to heating up the system, moves it away from ice/water co-existence conditions. When

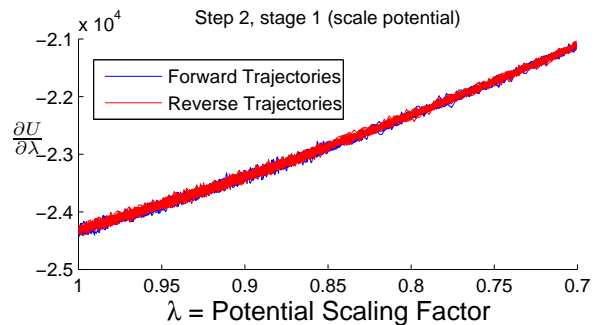


FIG. 4: Scaling the potential of the (uncleaved) water system. This is done at the beginning of step 2 before cleaving. The transition suffers from no hysteresis.

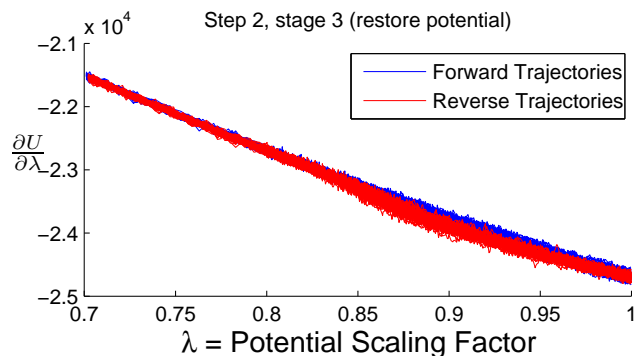


FIG. 5: Restoring the potential of the (cleaved) water system. This is done at the end of step 2 after cleaving. There is still some hysteresis, as the cleaved system approaches co-existence conditions, but the problem is far less severe than the cleaving hysteresis of figure 2.

the cleaving wells are introduced into a system with the potential reduced by 30%, there is no hysteresis, as can be seen in Figure 3. To calculate the cleaving free energy at co-existence conditions using this ‘potential scaling’ technique requires three separate stages:

- Reduce the interaction potential of the (uncleaved) water system by 30%
- Cleave the (reduced-potential) water system by introducing the wells
- Restore the potential of the (cleaved) water system to its full value

The free energy for each stage is calculated (using similar techniques as before), and the total free energy of cleaving at co-existence is the sum of the three individual free energies. Graphs are shown for reducing the potential (Figure 4), and restoring the potential (Figure 5). There remains some hysteresis in the final stage (restoring the potential), as the cleaved system approaches full-potential (and therefore co-existence conditions). Despite slowing down the trajectories in this region, a slight hysteresis is still present, although it is now far less severe

TABLE I: Duration of simulation runs in each step for the three interface orientations and the number of forward and reverse trajectories (in brackets) we ran in order to obtain the stated accuracy of our results.

	Basal	Prism	$\{11\bar{2}0\}$
Step 1	0.4 ns (10)	0.4 ns (5)	0.4 ns (10)
Step 2, heat	1.0 ns (10)	0.9 ns (15)	1.0 ns (10)
Step 2, cleave	2.4 ns (30)	1.7 ns (15)	1.8 ns (20)
Step 2, cool	2.6 ns (60)	4.4 ns (60)	4.9 ns (40)
Step 3	0.8 ns (20)	1.0 ns (25)	0.2 ns (5)
Step 4	1.3 ns (25)	1.3 ns (30)	0.8 ns (20)

than the original cleaving hysteresis, and the trajectories are close enough for free energy to be calculated with reasonable accuracy.

NUMBER AND SIMULATION TIME OF TRAJECTORIES

As discussed in the previous section, the simulation runs need to be slow enough in order for the nonequilibrium runs to stay relatively close to equilibrium. As can

be seen in Table I, in Steps 1, 2(heat), and 3, this was achieved with the much shorter runs than in other steps.

-
- [1] J. R. Morris and X. Song, *J. Chem. Phys.* **116**, 9352 (2002).
 - [2] J. Wang, S. Yoo, J. Bai, J. R. Morris, and X. C. Zeng, *J. Chem. Phys.* **123**, 036101 (2005).
 - [3] R. G. Fernández, J. L. F. Abascal, and C. Vega, *J. Chem. Phys.* **124**, 144506 (2006).
 - [4] Y. Koyama, H. Tanaka, G. Gao, and X. C. Zeng, *J. Chem. Phys.* **121**, 7926 (2004).
 - [5] C. Vega, E. Sanz, and J. L. F. Abascal, *J. Chem. Phys.* **122**, 114507 (2005).
 - [6] D. Frenkel and B. Smit, *Understanding Molecular Simulation: From Algorithms to Applications* (Academic Press, San Diego, 2002), 2nd ed.
 - [7] C. H. Bennett, *J. Comput. Phys.* **22**, 245 (1976).
 - [8] G. E. Crooks, *Phys. Rev. E* **61**, 2361 (2000).
 - [9] M. R. Shirts, V. S. Pande, E. Bair, and G. Hooker, *Phys. Rev. Lett.* **91**, 140601 (2003).
 - [10] R. L. Davidchack and B. B. Laird, *J. Chem. Phys.* **118**, 7651 (2003).
 - [11] R. L. Davidchack and B. B. Laird, *Phys. Rev. Lett.* **94**, 086102 (2005).